Development and experimental study of a 5kW cooling capacity ammonia-water absorption chiller

S. Bonnot[1], D. Triché[1], H. Demasles[1], F. Lefrançois[1], F. Boudéhenn[1] and J. Wytttenbach[1]

[1]CEA LITEN INES, 50 avenue du Lac Léman, 73370, Le Bourget du Lac, France

Abstract

A new and improved version of a low capacity ammonia-water absorption chiller was built and tested. This article presents how architecture and design optimization were performed to achieve enhanced performances compared to former prototype. The new chiller was first tested on an experimental test bench and then connected to an actual office air-conditioning system for a real solar cooling field test. The article shows, firstly a comparison between the former and the new chiller, secondly it presents a chiller's starting in nominal conditions and finally it develops chiller's performances according to operating temperatures on the experimental test bench. Results show better performances not only for cooling capacity and thermal COP but also for repeatability and general stability thanks to a re-engineered control strategy.

Key-words: ammonia-water absorption chiller, design, experimental results.

1. Introduction

In order to reduce global CO_2 emissions and energy consumption while the demand of air conditioning in building rises strongly (Pons et al., 2012), the use of renewable energy becomes essential. Due to the strong correlation between availability of solar resource and building cooling demand (Lecuona et al., 2009), this energy seems to be one of the most interesting ways for air-conditioning. From this perspective, a prototype of low cooling capacity (5 kW) ammonia-water absorption chiller designed for solar applications was built in 2010 (Boudéhenn et al., 2012). It was designed with only plate heat exchangers, to reduce both cost and ammonia charge and was widely instrumented. This prototype proved the feasibility of such technology with satisfactory thermal COP and cooling capacity. A new version of the chiller was developed in 2013 with the following criteria: better compactness, fewer instrumentation and with design improvements. This system is to be installed on a solar air conditioning facility instead of a commercial LiBr-H_2O absorption chiller. This paper presents the development of this second chiller, explaining its architecture and analyzing its performances.

2. Technical choices and design

The new chiller is based on the previous one with similar features (Fig. 1). It's composed of 6 plate heat exchangers: the usual generator, absorber, evaporator, and condenser; a solution heat exchanger located between rich and poor solution; and a rectification exchanger.

The flat plate heat exchanger technology was used because of its compactness; this technology allows the reduction of fluid quantity and is supposed to be less expensive for a future industrial product.

The rectification exchanger works by partial condensation of the refrigerant with external cooling.

The subcooler, which usually sub-cools or superheats refrigerant before and after the evaporator (Boudéhenn et al., 2012), has been removed since its effect wasn't economically interesting.

Four tanks are used. Two of them perform liquid-vapor separation, firstly to separate ammonia vapor from poor solution at the outlet of the generator (T2) and secondly to separate ammonia vapor from condensates at

the rectification exchanger outlet (T3). In these two cases, the poor solution or the condensates are reinserted into the poor solution circuit. The other two tanks are used for storage. They provide a buffer between the condenser and the evaporator (T4) and between the absorber and the solution pump (T1). External temperatures variations lead to the variation of rich and poor solutions concentrations and the two tanks allow the compensation of concentration variations in the solutions according to temperatures. The tank after the absorber stores rich solution and the tank after condenser stores ammonia. Indeed, according to concentration of poor solution and refrigerant vapor, the cycle needs more or less ammonia and water.

Pump used to transfer solution from absorber to generator is a diaphragm pump coupled with a variable speed motor, which enables the cooling power to vary and the machine to start gradually.

Two electronic expansion valves are used to control and regulate the chiller. The first expansion valve is located before the evaporator and adjusts superheating at the outlet of the evaporator. Superheating is the difference between evaporation temperature and the temperature at the outlet of the evaporator. To increase superheating, the expansion valve must be used to reduce the refrigerant flow in order to increase the evaporation process as well as the temperature at the outlet of the evaporator. The other control valve is located between the solution heat exchanger and the absorber and adjusts the liquid level in the separation tank at the outlet of the generator, comparing it to setpoint. There is an optimal position of the control valve to maintain the level on the separation tank; it depends on solution mass flow rate and pressure drop.

The control strategy has been improved as follows: instructions on superheating value and liquid level in the separation tank have been established and fixed in order to stabilize the chiller's performance whatever the operating temperatures and the two PID controllers have finely been adjusted.
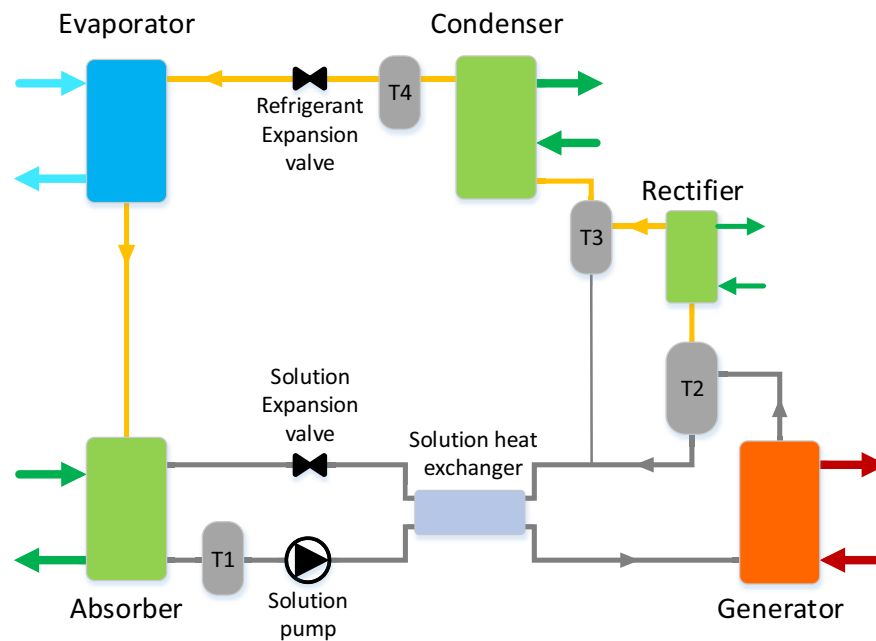

Fig. 1: Chiller operating diagram

The chiller is less instrumented than the former prototype because it is a pre-industrial version intended to be coupled with a real solar cooling plant at INES (French National Institute for Solar Energy) facility (Cheze et al., 2011). However, it is still equipped with various sensors, especially, for control strategy. The sensors are quantified and described in Table 1.

Tab. 1: Sensors number and measurement characteristics

Sensors type	Number	Uncertainty (+/-)
Heat transfer fluid temperature (Pt)	6	0.1K
Refrigerant temperature (TC) (fixed on the wall)	13	0.3K
Refrigerant pressure (0-10bar and 0-25bar)	2	0.2% full scale
Liquid level (capacitive)	2	0.5%

Ammonia being a very corrosive fluid, especially with water, a close attention has been paid to all material in contact with the fluid, using as far as possible stainless steel and EPDM or PTFE for seals and membranes.

Since this chiller is a pre-industrial version, a particular attention was paid to ensure the compactness of each part of the chiller in order to reduce the overall size of the engine (Fig. 2).

Fig. 2: Pictures of the new chiller and its cover

Fig. 3: Picture of the former prototype

Compared to the previous chiller (Fig. 3), overall inner volume has been reduced by shortening pipes, removing instrumentation and limiting operating temperature range. The chiller has been completely rethought and redesigned. These modifications lead to decrease ammonia charge from 2.4 kg to 1.8 kg for

the same cooling capacity (5 kW) and water quantity from 0.89 kg to 0.85 kg. The refrigerant charge is close to 0.36 kg per kW, which is lower than all commercial chillers. There is no installation restriction because the ammonia charge is less than 2.5 kg (according to NF EN 378) and therefore, the chiller can be installed inside a building or a room without any specific safety system. The efforts made to reduce the overall size have enabled to create a very compact chiller of 0.36 m^3 weighing 106 kg.

Efforts have also been made in terms of visual aspect and usability. A work has been made on the design of the metallic structure that covers the machine and a touch screen has been added in order to control the chiller and to visualize its performances (Fig. 4).

Fig. 4: Touch screen to control the chiller

3. Results and comparison

As the previous one, tests were performed at INES experimental facility providing adjustable power and temperature levels for cooling or heating on the ports of the chiller. The chiller was tested on ranges of external temperatures and solution mass flow as shown on Table 2, and more than 80 tests in steady state conditions were performed.

Tab. 2: Operating conditions

	Minimum	**Nominal**	**Maximum**
Temperature generator inlet	60°C	80°C	95°C
Temperature evaporator inlet	9°C	18°C	18°C
Temperature absorber-condenser inlet	23°C	27°C	33°C
Pump mass flow	45 kg/h	84 kg/h	90 kg/h

3.1. *Performance enhancement*

At nominal inlet conditions, first tests have shown that the thermal COP (COP$_{th}$) is 0.64 and the cooling capacity (Q_E) is 5.1 kW in steady-state conditions. The thermal COP is defined as the ratio between cooling and heating power. Compared to the previous chiller, values of COP$_{th}$ and Q_E are better. This highlights the improvement of the components, and the less scattered dots (Fig. 5) show the effect of controls improvements.

Fig. 5 stresses that repeatability and stability on the former prototype (chiller 1) are insufficient. Indeed, for the same inlet conditions and the same pump mass flow, chiller 1 COP values vary from 0.5 to 0.65 and its cooling capacity values range from 3.5 kW to 4.2 kW. On the contrary, chiller 2 (new one) COP and cooling capacity values are more coherent, reliable and repeatable thanks to the improved control strategy.

First of all, chiller 2 values show that thermal COP does not depend on pump mass flow. Whatever the pump mass flow, the thermal COP remains constant.

Then, chiller 2 values emphasize that cooling capacity is proportional to the pump mass flow. To be more accurate, the cooling capacity increases linearly until 85 kg/h, but then it remains constant.

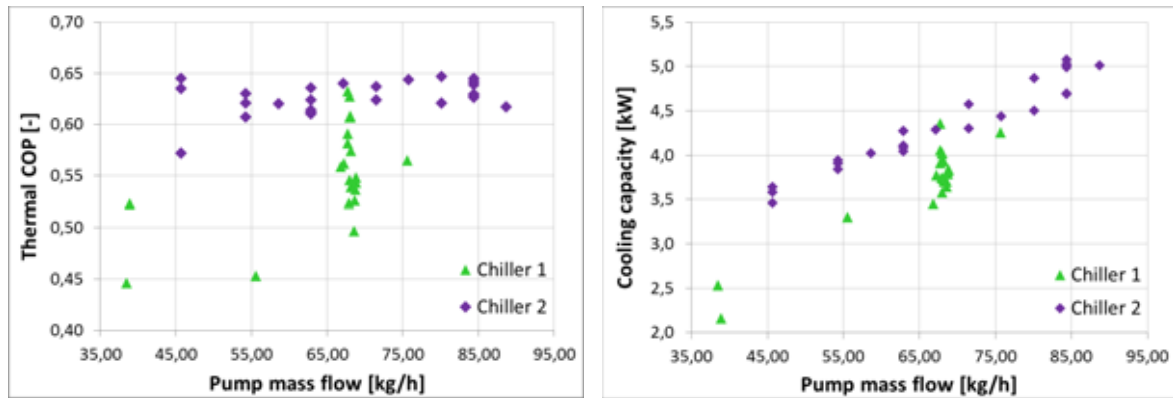Therefore, strongly increase the pump mass flow is not required.

Fig. 5: Comparison of thermal COP and cooling capacity between the 2 chillers for nominal temperatures

3.2. *Starting of the chiller*

Automated control improvement and variable pump speed allow a very fast starting. Fig. 6 shows a starting at nominal temperature conditions with a gradual increase of pump speed from 30% to 50%.

The chiller is switched on at t = 0 min. Then, 7 minutes later, the cooling capacity reaches a value equal to the steady-state, and after a little overshoot, the chiller stabilizes on steady state after 22 minutes.

As flow control by expansion valves is faster and has more impact with low mass flow rates, gradual increase of pump speed reduces starting time by limiting oscillations and transient state, and prevents from emptying tanks, which is usual at starting.
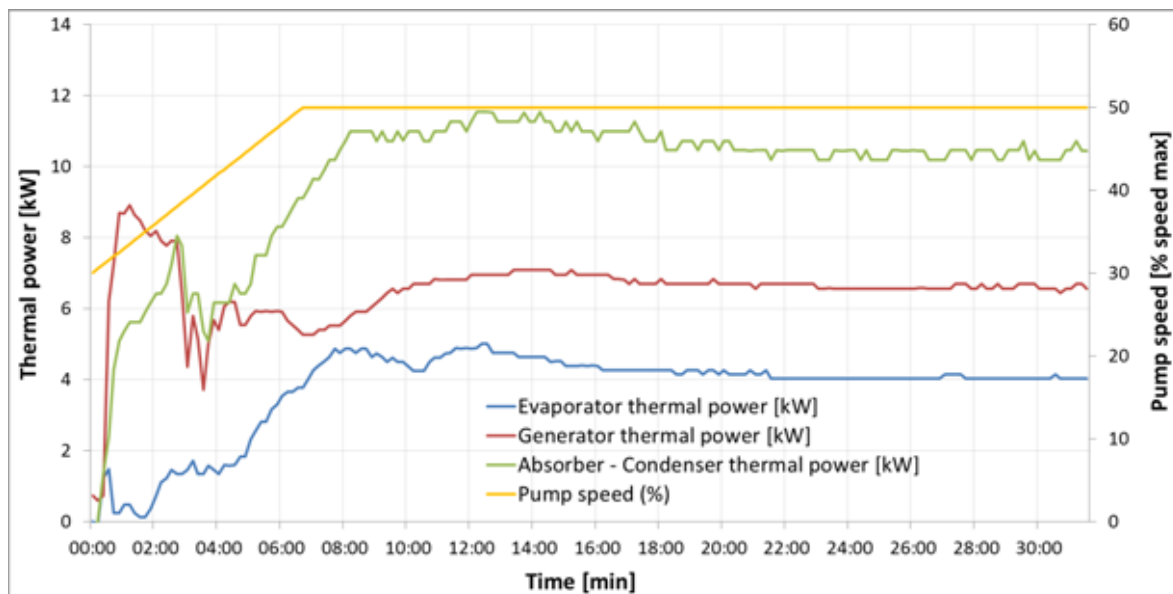

Fig 6: Starting in nominal conditions

Fig. 6 shows standard patterns occurring at starting: The first peak on generator power curve is explained by global warm-up of the machine, and the low oscillations on all power curves are due to high variations of expansion valves at starting before reaching a steady position.

3.3. *Temperature impacts*

The following graphs (Fig 7, 8, 9) show thermal COP and cooling capacity evolution when operating temperatures change. For each operating condition, the average over 15 minutes of steady state is represented by a dot.
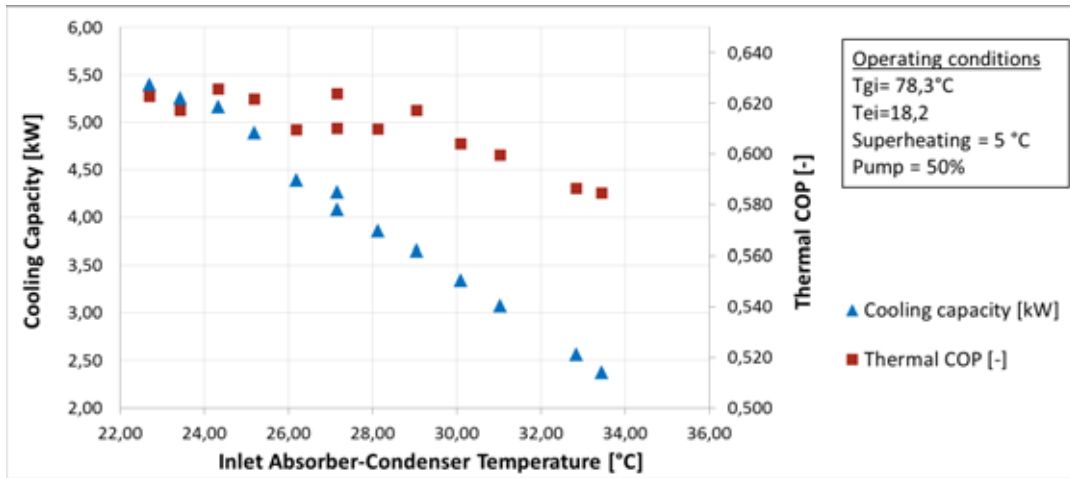
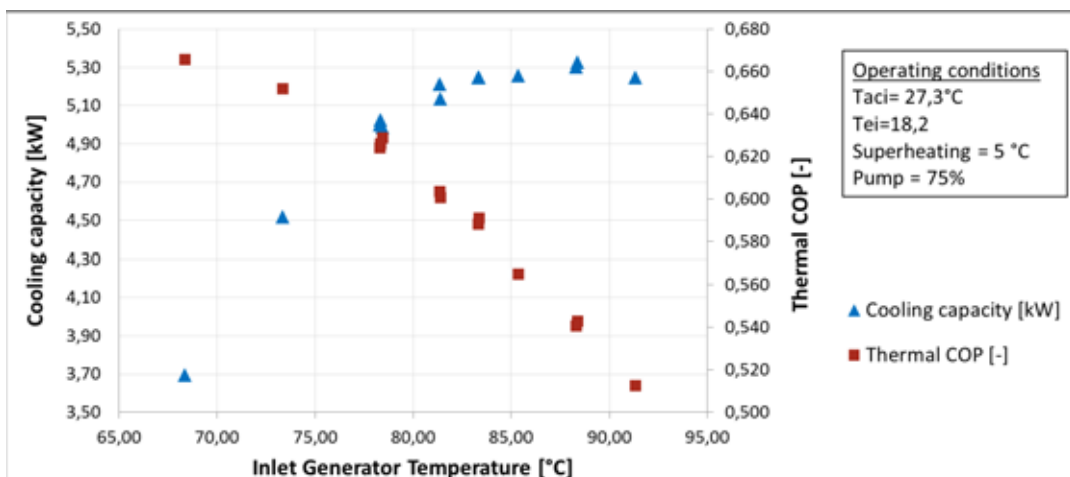**Fig 7: Impact of Absorber-Condenser temperature on thermal COP and cooling capacity**

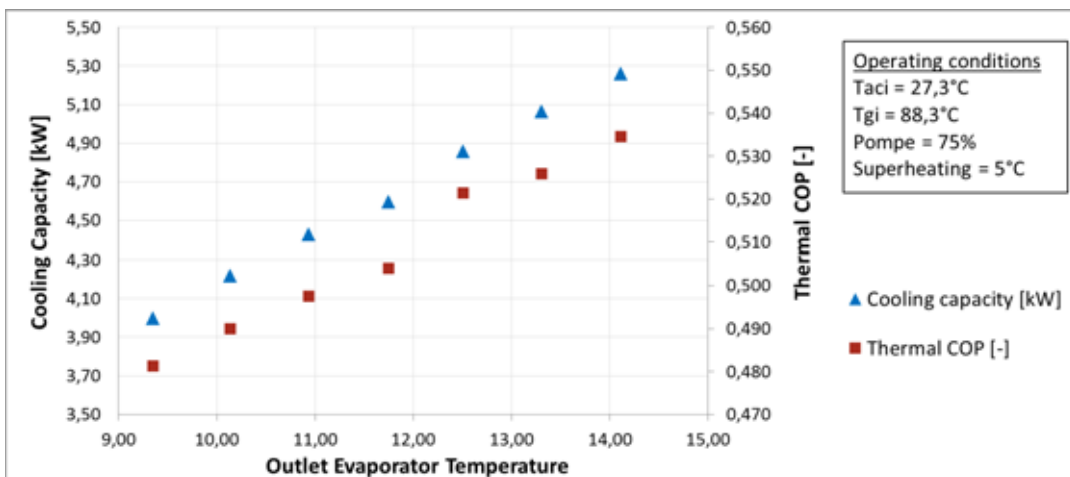**Fig 8: Impact of Generator temperature on thermal COP and cooling capacity**

Fig 9: Impact of Evaporator temperature on thermal COP and cooling capacity

Impacts of temperature variations are summed up in the following table (Tab. 3).

Tab. 3: Temperatures variations to improve performances

	Generator Temperature	Absorber - Condenser Temperature	Evaporator Temperature
To increase COP$_{th}$	↘	↘	↗
To increase Q$_{evap}$	↗	↘	↗

Absorber-Condenser temperature should be set as low as possible, and evaporator temperature as high as possible to improve performances of the chiller, according to Carnot efficiency definition.

Generator temperature impact is the opposite for COP$_{th}$ and cooling capacity. The impact of the generator temperature on the thermal COP does not follow Carnot efficiency definition trend. Indeed, thermal COP should increase according to generator temperature and over a value, it should remain constant.

The decrease of thermal COP according to generator temperature is owed to the architecture of the machine and its irreversibilities. The calculation of the chiller exergetic efficiency is required in order to take into account machine's irreversibilities. Exergetic efficiency is defined as follows (Sözen, 2001):

$$\eta_{ex} = \frac{-P_E \left(1 - \frac{T_0}{T_e}\right)}{P_G \left(1 - \frac{T_0}{T_g}\right) + W} \qquad (eq. 1)$$

Absorber condenser temperature is the reference temperature (T_0).

The work of the solution pump (W) can be neglected and exergetic efficiency can be simplified as follows:

$$\eta_{ex} = \frac{COP_{th}}{COP_{carnot}} \qquad (eq. 2)$$

So, there is an optimal generator temperature which provides the maximal exergetic efficiency. Therefore, generator temperature increase should be limited in order to maintain chiller's efficiency.

If this temperature can be controlled, it should be set to the lowest value that allows producing the desired cooling capacity, in order to keep the thermal COP as high as possible.

4. Conclusion and perspectives

This article presents a new and improved version of a low capacity ammonia-water absorption chiller for solar cooling application. The objectives of compactness, low ammonia charge, reliability, repeatability and stability led to re-engineer the control strategy, to remove instrumentation and to work on a new design compared to the former prototype. Regarding heat exchanger technology, flat plate heat exchangers were selected since they proved to be promising with the previous prototype.

Experimental results of the new chiller at INES test facility show better performances compared to the former prototype. The reliability of the chiller is much more satisfying. Besides, the machine starts easily and quickly.

Nevertheless, further optimization points have been identified, especially regarding the absorption, desorption and rectification processes. A study on coupled heat and mass transfers during these processes is in progress.

Now that experimental results show a good stability, the new chiller has been coupled with an actual office air-conditioning system for a real solar cooling field test.

The installation (Fig. 10) is composed of the absorption chiller, a cold storage tank, a hot storage tank, 30 m^2 flat plate solar collector field on the rooftop and a heat rejection ground loop (Chèze et al., 2011).

Fig 10: View of operating installation

The objective is to find the same reliable results under real rather than controlled operating conditions.

5. Nomenclature

Quantity	Symbol	Unit
Coefficient of performance	COP	
Platinum resistance thermometer	Pt	
Power	P	[W]
Cooling capacity	Q_E	[kW]
Thermocouple	TC	
Temperature	T	[°C]
Reference temperature	T_0	[°C]
Work of the pump	W	[W]
Efficiency	η	[-]
Subscripts	Symbol	
Generator inlet	gi	
Generator	G, g	
Evaporator inlet	ei	
Evaporator	E, e	
Exergetic	ex	
Absorber-condenser inlet	aci	
Evaporator	evap	
Thermal	th	

6. References

Boudéhenn, F., Demasles, H., Wyttenbach, J., Jobard, X., Chèze, D., Papillon, P., 2012. Development of a 5 kW Cooling Capacity Ammonia-water Absorption Chiller for Solar Cooling Applications. Energy Procedia, 30, 35 – 43.

Chèze, D., Boudéhenn, F., Papillon, P., Mugnier, D., Nunez, T., 2011. Solera demonstrator of small scale solar heating and cooling system in INES office building, 3th International Conference Solar Air-Conditioning proceedings, Larnaca, Cyprus.

Lecuona, A., Ventas, R., Venegas, M., Zacarias, A., Salgado, R. 2009. Optimum hot water temperature for absorption solar cooling. Solar Energy, 83, 1806-1814.

Pons, M., Anies, G., Boudéhenn, F., Bourdoukan, P., Castaing-Lasvignottes, J., Evola, G., Le Denn, A., Le Pierres, N., Marc, O., Mazet, N., Sitout, D., Lucas, F., 2012. Performance comparison of six solar-powered air-conditioners operated in five places. Energy, 46, 471-483.

Sözen, A., 2001. Effect of heat exchangers on performance of absorption refrigeration systems. Energy Conversion and Management, 42, 1699-1716.

NF EN 378 – Refrigeration systems and heat pumps – Safety and environment requirements. French and European standard.